JOURNAL OF MATERIALS SCIENCE **34** (1999) 4931–4936

The crack tip strain field of AISI 4340

Part III *Hydrogen influence*

N. N. KINAEV
Department of Mining, Minerals and Materials Engineering, The University of Queensland, Brisbane, QLD, 4072
Centre for Microscopy and Microanalysis, The University of Queensland, QLD, 4072

D. R. COUSENS
Centre for Microscopy and Microanalysis, The University of Queensland, QLD, 4072

A. ATRENS*
Department of Mining, Minerals and Materials Engineering, The University of Queensland, Brisbane, QLD, 4072
E-mail: atrens@minmet.uq.oz.au

This paper studied the influence of hydrogen and water vapour environments on the plastic behaviour in the vicinity of the crack tip for AISI 4340. Hydrogen and water vapour (at a pressure of 15 Torr) significantly increased the crack tip opening displacement. The crack tip strain distribution in 15 Torr hydrogen was significantly different to that measured in vacuum. In the presence of sufficient hydrogen, the plastic zone was larger, was elongated in the direction of crack propagation and moreover there was significant creep. These observations support the hydrogen enhanced localised plasticity model for hydrogen embrittlement in this steel. The strain distribution in the presence of water vapour also suggests that SCC in AISI 4340 occurs via the hydrogen enhanced localised plasticity mechanism.

1. Introduction

Kinaev *et al*. [1, 2] showed that the crack-tip strain field for AISI 4340 high strength steel exhibited significantly more plasticity than expected from continuum plasticity as embodied in the HRR model [3–5]. Moreover, there is little direct experimental data on the influence of hydrogen and water vapour on the crack tip strain field for AISI 4340 steel. The literature data are mutually contradictory. Davidson [6] found that for plain carbon steel hydrogen suppressed plasticity at the crack tip and promoted embrittlement. In contrast, Sun *et al*. [7] found hydrogen enhanced plasticity in FCC nickel single crystals. The present work examined the influence of hydrogen and water vapour on the crack tip strain field for AISI 4340 steel.

2. Experimental

The sample materials, sample geometry and sample preparation were described previously by Kinaev *et al*. [1]. Furthermore, the ESEM configuration and operation procedure for the experiments in hydrogen were also as described by Kinaev *et al*. [1].

Three sets of experiments were carried out to study the strain distribution at the crack tip for AISI 4340 high strength steel in hydrogen. The first series (performed on sample AH) was carried out with a constant hydrogen pressure of 5 Torr. The applied stress intensity factor K_I was increased during the experiment as shown in Fig. 1. This series was performed to measure the CTOD in a hydrogen environment relative to the CTOD in a pure fracture mechanics situation (as for the experiments in high vacuum as described by Kinaev *et al*. [1]). In the second series (sample BH), the sample was loaded to a stress intensity factor K_I of 20 MPa$\sqrt{m}$ and maintained in a hydrogen atmosphere at a pressure of 5 Torr for 3 h. The hydrogen atmosphere was then replaced with water vapour at a pressure of 5 and subsequently 15 Torr. This series aimed firstly to determine the crack tip strain field in a low pressure of hydrogen, and secondly to observe the influence of water vapour. The third series (sample CH) measured the crack tip strain distribution at the higher hydrogen pressure of 15 Torr. The sample was loaded to an applied stress intensity factor K_I of 25 MPa$\sqrt{m}$ at a hydrogen pressure of 15 Torr and was held under these conditions for 6.5 h.

3. Results

3.1. Crack front

The samples were broken open after the strain mapping as described by Kinaev *et al*. [2] and the shape of the crack front on the fracture surface examined for each

* Author to whom all correspondence should be addressed.

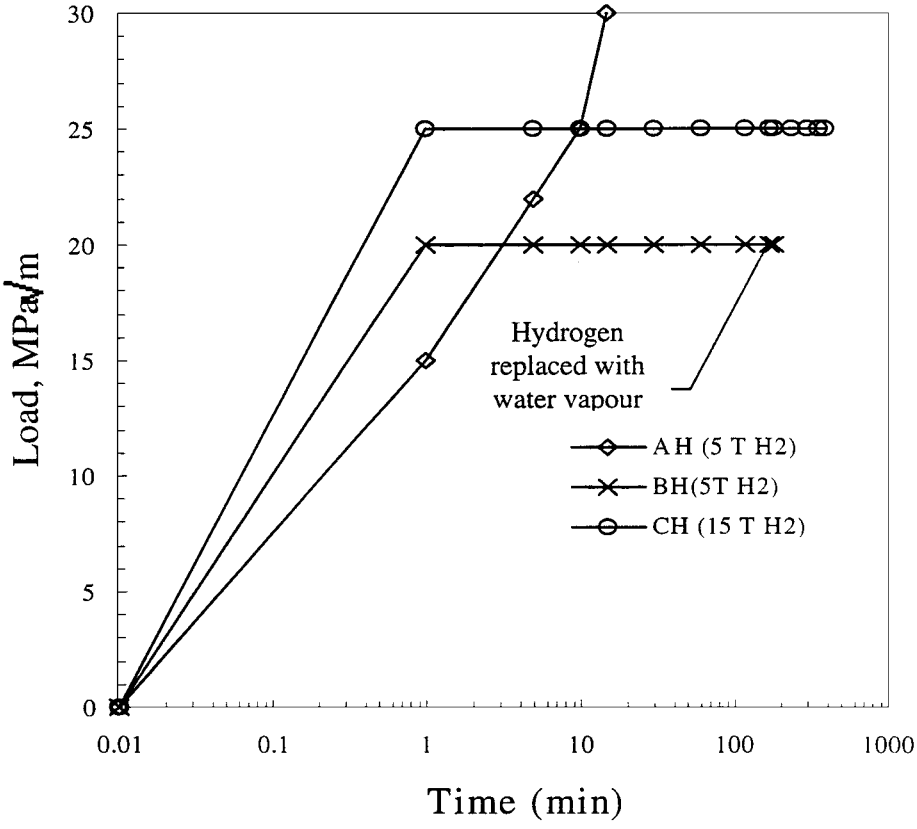

Figure 1 Loading scheme for the experiments in hydrogen.

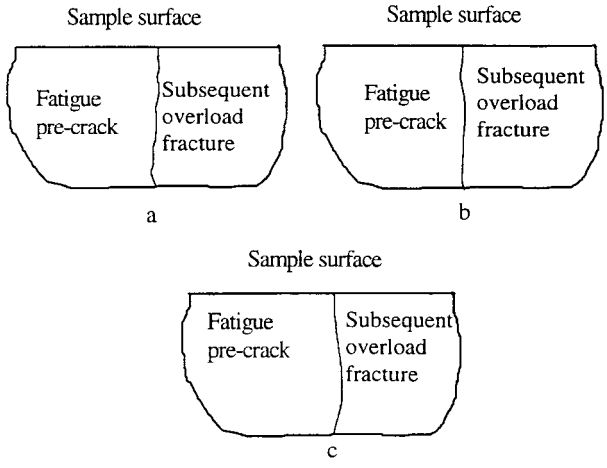

Figure 2 Shape of the fatigue pre-crack profile as visible on the fracture surface after breaking the specimen open after the experiments for series (a) AH (b) BH (c) CH.

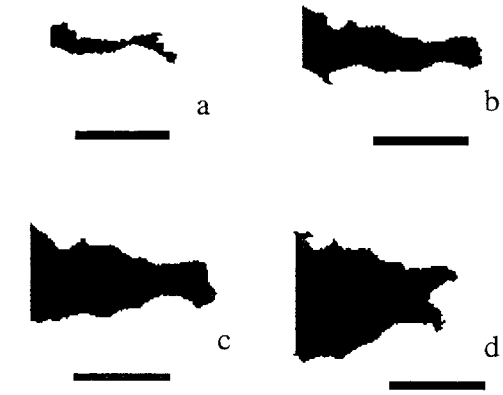

Figure 3 Cross-sectional shape of the crack tip of the AH (5 Torr H_2) sample for the following values of the stress intensity factor K_I (a) 15 MPa$\sqrt{}$m; (b) 22 MPa$\sqrt{}$m; (c) 25 MPa$\sqrt{}$m; (d) 30 MPa$\sqrt{}$m. In each case the scale bar has a length of 10 μm.

sample. As illustrated in Fig. 2, in all three samples the crack front was almost perpendicular to the observed surface. This allowed the use of the results from all the experiments without any need for corrections for crack tunnelling.

3.2. Crack tip shape and crack tip opening displacement

Typical crack tip cross-sectional shapes are presented in Figs 3–5. In the hydrogen environments the crack tips tended to remained single and had only a small tendency for crack branching, unlike the crack tips in the experiments in high vacuum (Kinaev *et al.* [2]) where there was usually significant crack branching, However,

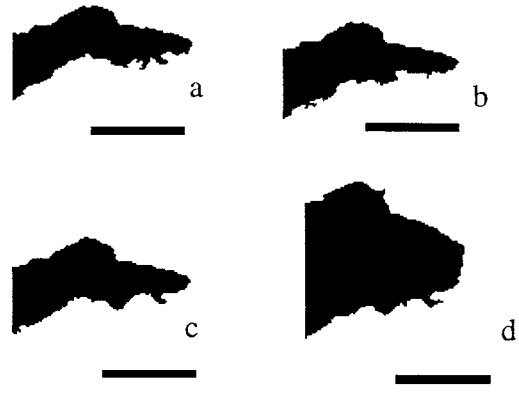

Figure 4 Cross-sectional shape of the crack tip of BH sample (a) 10 min after loading to 20 MPa$\sqrt{}$m in 5 Torr H_2; (b) 60 min after loading; (c) 170 min after loading; and (d) after replacing the hydrogen environment with water vapour. In each case the sacle bar has a length of 10 μm.

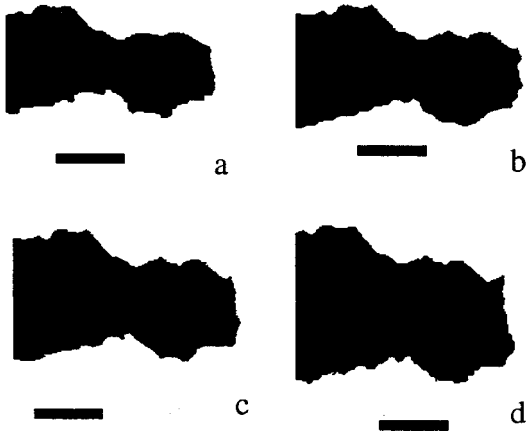

Figure 5 Cross-sectional shape of the crack tip of the CH sample (25 MPa$\sqrt{m}$ in 15 Torr H_2) (a) 6 min after loading; (b) 60 min after loading; (c) 125 min after loading; (d) 180 min after loading. In each case the sacle bar has a length of 10 μm.

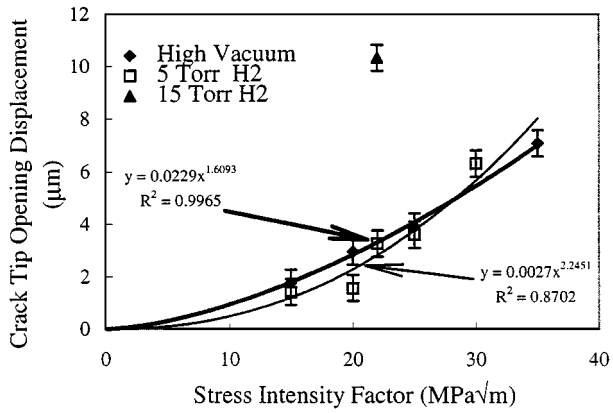

Figure 6 Dependence of CTOD on applied stress intensity factors and environment.

there was some crack branching for high values of applied stress intensity factor at 5 Torr hydrogen (see Fig. 3d) and after several hours of exposure under load at the higher pressure of hydrogen (Fig. 5d). Time dependent crack blunting was observed in most cases, although no crack propagation was detected. The replacement of the hydrogen environment with water vapour resulted in significant crack tip blunting (Fig. 4d).

Initial values of CTOD for the experiments in 5 Torr of hydrogen were comparable with the values measured in high vacuum (Fig. 6). In contrast, the initial value of CTOD in 15 Torr of hydrogen was almost three times higher than the corresponding value in high vacuum.

The time dependence of the CTOD for different hydrogen pressures are presented in Fig. 7. For a hydrogen pressure of 5 Torr, the CTOD remained essentially unchanged for almost 2 h. Replacing the hydrogen environment with water vapour at the same pressure resulted in a slight increase of the CTOD. A further increase in the pressure of water vapour to 15 Torr resulted in an increase of the CTOD to almost three times the initial value.

The CTOD in 15 Torr hydrogen was initially significantly larger than the CTOD at 5 Torr. The increase in the CTOD accelerated approximately 30 min after sample loading and within 3.5 h the CTOD had increased to

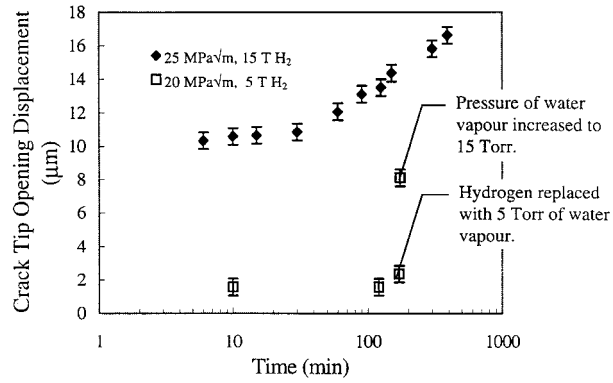

Figure 7 Time dependence of the CTOD.

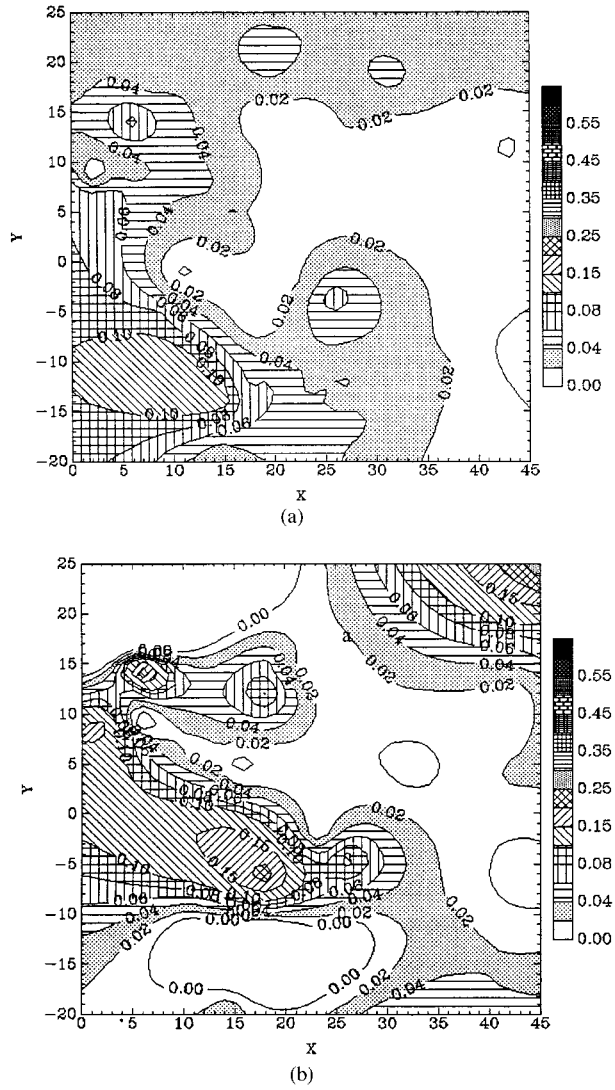

Figure 8 ε_{yy} strain field for the BH sample at an applied stress intensity factor K_I of 20 MPa$\sqrt{m}$ (a) 10 min after loading at 5 Torr of H_2 and (b) 3 min after replacing hydrogen with 15 Torr of water vapour.

almost 2 times its starting value. The time dependence of the CTOD indicated the occurrence of the creep.

3.3. ε_{yy} Strain field

Typical examples of the ε_{yy} crack tip strain field are presented in Figs 8 and 9. For the BH sample, the ε_{yy} strain field in the vicinity of the crack tip 10 min after

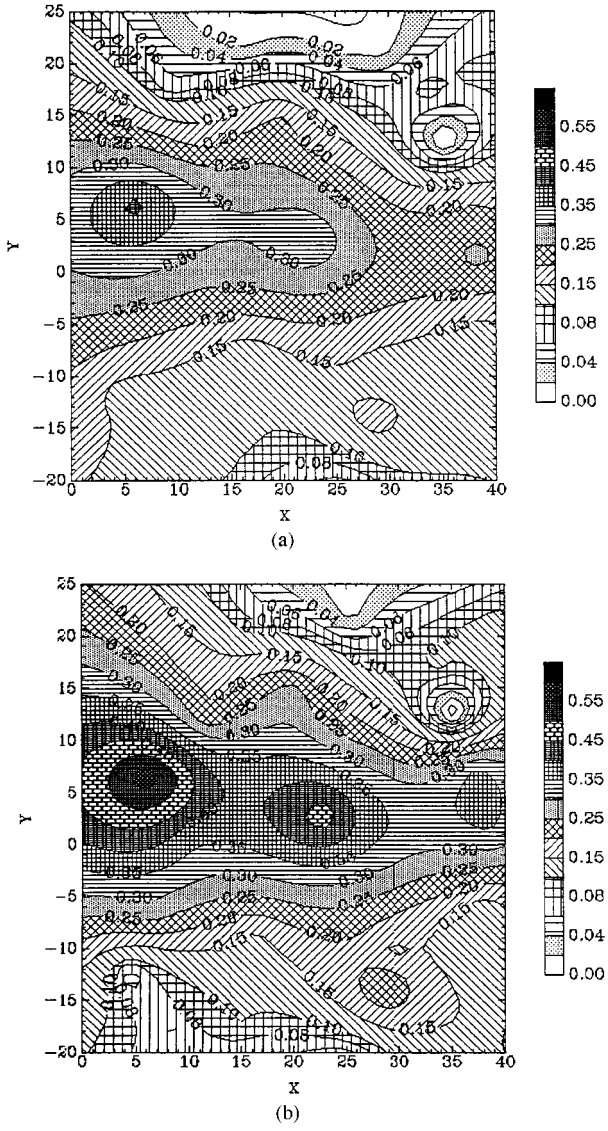

Figure 9 ε_{yy} strain field for the CH sample at an applied stress intensity factor K_I of 25 MPa$\sqrt{m}$ and 15 Torr of H_2 (a) 10 min after loading; (b) 180 min after loading.

the loading in 5 Torr H_2 (Fig. 8a) was comparable with the strain field measured at the same applied stress intensity factor in high vacuum. This strain field may be characterised as having ridges, with high strain values in the directions of between 40° and 50° to the crack propagation direction. However, the size of the plastic zone where the strain was higher than 0.02 was significantly higher than both the HRR prediction and the plastic zone measured in the high vacuum experiments (Kinaev *et al.* [2]). Also, the ε_{yy} strain values within this plastic zone were considerably larger than the values measured in high vacuum. There was little change in the crack tip strain field during several hours of loading in 5 Torr of hydrogen.

However, 3 min after replacing the hydrogen environment with water vapour at 15 Torr, the strain field had changed significantly (Fig. 8b). The strain ridge in the lower part of the map rotated towards the direction of crack propagation. Consequently, the angle between the strain ridge and the direction of the crack growth decreased. The size of the plastic zone also increased.

The ε_{yy} strain field measured at a higher pressure of hydrogen (15 Torr) and a similar applied stress intensity factor (sample CH) showed a significantly different pattern, as illustrated in Fig. 9. The ε_{yy} strain field measured 10 min after loading (Fig. 9a) was elongated along the direction of crack propagation, the length of the plastic zone was significantly larger and the strain values considerably larger. The general character of the ε_{yy} strain field did not change significantly for 3 h after loading, but the strain values increased (Fig. 9b). For example, the maximum ε_{yy} strain value located at the point ($x = 6$ μm, $y = 6$ μm) increased from 0.45 (10 min after loading) to almost 0.60 (180 min after loading). Another notable change with time in the strain field was the appearance of an island of high ε_{yy} strain 20 μm ahead of the crack, and also the appearance of a strain ridge with the same orientation to the BH sample which originated approximately 15 μm ahead of the crack tip.

3.4. Total effective strain ε_{ef} field

The distribution of the total effective strain ε_{ef}, for the BH and CH samples are presented in Figs 10 and 11. The total effective strain ε_{ef} for the BH sample 10 min after loading (Fig. 10a) showed a strain ridge in a

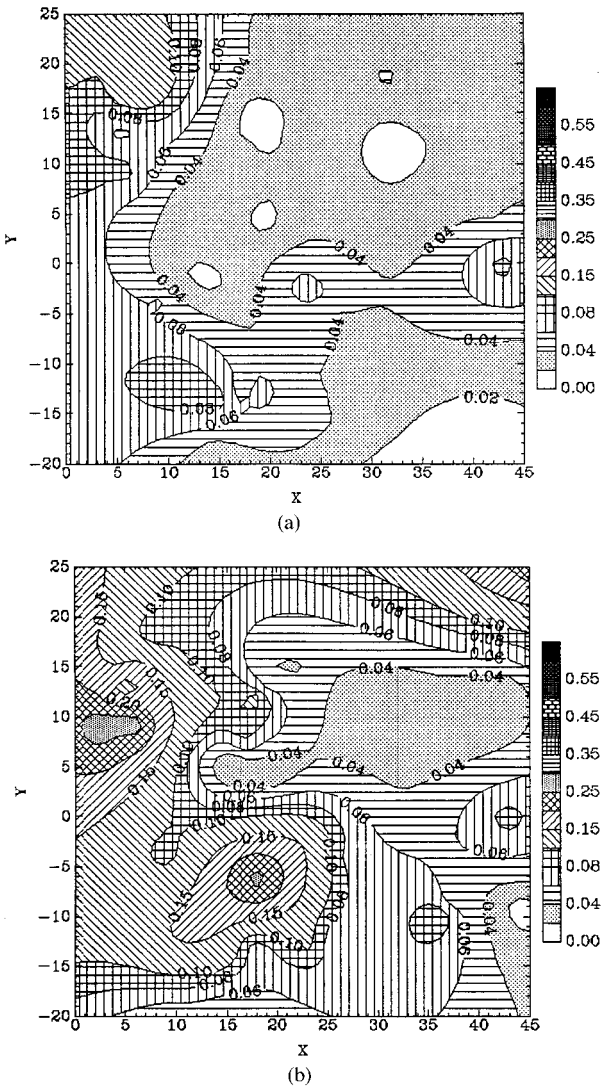

Figure 10 ε_{ef} strain field for the BH sample at an applied stress intensity factor K_I of 20 MPa$\sqrt{m}$ (a) 10 min after loading at 5 Torr of H_2 and (b) 3 min after replacing hydrogen with 15 Torr of water vapour.

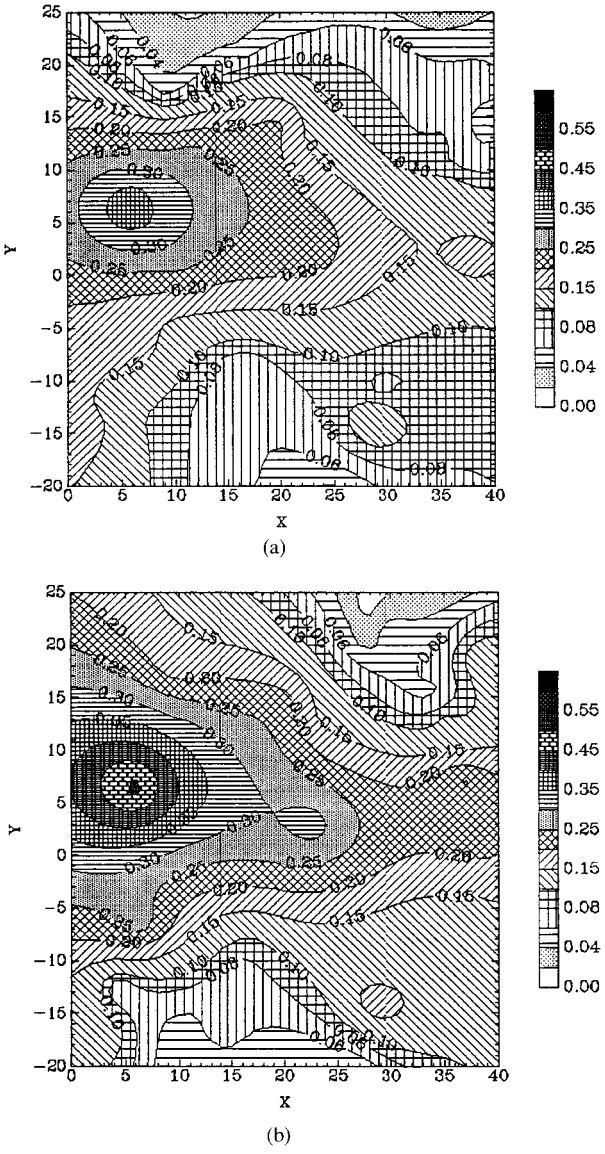

(a) (b)

Figure 11 ε_{ef} strain field for the CH sample at an applied stress intensity factor K_I of 25 MPa$\sqrt{m}$ and 15 Torr of H_2 (a) 10 min after loading; (b) 180 min after loading.

direction of between 50° and 75° to the direction of the crack propagation. The ridge in the lower part of the strain map had a maximum strain value of 0.08 located at the point $x = 10$ μm, $y = -10$ μm.

Changing the environment from 5 Torr hydrogen to 15 Torr water vapour significantly altered the strain distribution (Fig. 10b). The ridge in the lower part of the strain map became significantly wider and its orientation changed to approximately 30° relative to the *X*-axis. The maximum value of strain increased almost threefold (from 0.08 to 0.25). The location of the maximum strain shifted to the point at $x = 17$ μm, $y = -7$ μm. The upper section of the strain map also had several changes. The maximum of the strain in this part of the strain field was closer to the crack at a point with coordinates of $x = 5$ μm, $y = 8$ μm. The value of the maximum strain increased from approximately 0.12 to 0.25.

The CH sample at a higher hydrogen pressure and a slight higher applied stress intensity factor had a significantly different total effective strain field. At 10 min after loading (Fig. 11a) the total effective strain was

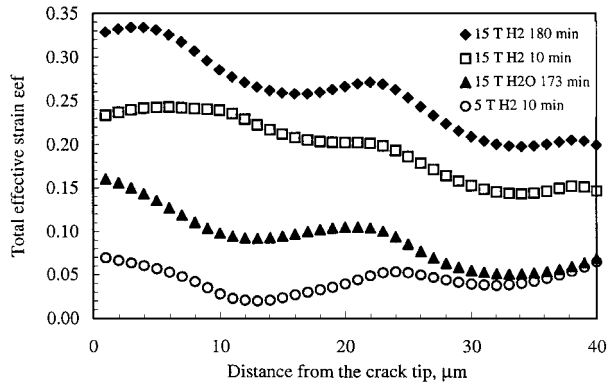

Figure 12 Distribution of the total effective strain ε_{ef} along the direction of a crack growth.

elongated along the crack propagation direction. The size of the plastic zone was also significantly larger than both the HRR model and high vacuum experiments (Kinaev *et al.* [2]). The point of a maximum total effective strain value of 0.35 was located at a same point ($x = 6$ mm, $y = 6$ mm) as for the ε_{yy} strain.

Holding the sample under load in 15 Torr of hydrogen resulted in changes to the total effective strain pattern similar to the changes of the tensile ε_{yy} strain (Fig. 11b). The strain field became more elongated along the direction of crack propagation. Although no crack growth was observed, the maximum total effective strain value increased from 0.35 to 0.5 without a change in the position of the maximum. Additional high strain values appeared approximately 22 μm ahead of the crack tip.

The total effective strain ε_{ef} along the direction of crack growth is presented in Fig. 12. The strain measured at the higher pressure of hydrogen was significantly higher than that measured at the lower pressure. Replacing hydrogen with water vapour at a higher pressure (BH sample) resulted in a significant increase in strain close to the crack tip. However, the values of total effective strain at distances larger than 30 μm were the same for 5 Torr hydrogen and 15 Torr water vapour. For a hydrogen pressure of 15 Torr (CH sample), changes with time showed a nearly constant increase in the total effective strain along the total observed distance.

4. Discussion

The strain distribution at the crack tip for AISI 4340 steel in hydrogen was very different to that measured in high vacuum. The major features of the strain distribution in a hydrogen environment were:

- The lower tendency to crack tip branching;
- The time dependence of the strain distribution and of CTOD;
- The high values of ε_{yy} and total effective strain ε_{ef};
- The large size of the plastic zone at the crack tip;
- The strong elongation of the strain field in the crack direction.

These observations indicate that hydrogen enhances the plasticity in the crack tip area. Indeed, the higher plasticity in the vicinity of the crack tip should depress

crack tip branching at small loads, resulting in crack tip blunting. The presence of creep in the experiments in hydrogen also indicates hydrogen enhanced plasticity. Further evidence of hydrogen enchanced plasticity comes from the values of strain measured in the hydrogen atmosphere experiments which were significantly higher than the ones measured in high vacuum. Elongation of the strain field along the crack propagation direction is in good agreement with expectations of the hydrogen enhanced local plasticity mechanism.

Hydrogen effects were dependant on the pressure of hydrogen. At a hydrogen pressure of 5 Torr (AH), the CTOD was similar to that in the high vacuum experiments (Fig. 6) and the increase in the CTOD with time was negligible. However, the magnitude of the strain in the vicinity of the crack tip and the size of the plastic zone were significantly higher than in high vacuum. Thus, at a relatively low pressure, hydrogen did not change the shape of the strain field and did increase the strain values without causing significant changes in the CTOD.

The behaviour was different at the hydrogen pressure to 15 Torr. The initial value of the CTOD almost tripled in comparison to that in high vacuum and in lower pressure environments and moreover there were significant increases of CTOD with time. At the higher pressure, the changes in strain distribution were larger. It may be assumed that a threshold hydrogen pressure exists, i.e. below a critical pressure, hydrogen is not the overriding influence on the strain distribution at the crack tip. As the hydrogen pressure increased, a larger quantity of hydrogen entered the steel and consequently had a greater effect on the mechanical properties of the steel. A pressure of 15 Torr of hydrogen at a stress intensity factor of 25 $MPa\sqrt{m}$ resulted in hydrogen enchanced plasticity at the crack tip.

The shape of the CTOD time curve suggests that after a certain time, the hydrogen induced changes in the plastic behaviour accelerate. At the current stage of experimental knowledge it is difficult to draw a definite conclusions concerning the possibility that the hydrogen partial pressure has a threshold value for the changes in the plasticity of AISI 4340 steel or if it only changes the kinetics of the process.

The water vapour environments also caused a similar influence on the plastic behaviour at the crack tip. An increase in the partial pressure of water vapour promoted changes in the strain field similar to those measured for the hydrogen environment. The similarities in the influence of water vapour and hydrogen on the plastic behaviour provides grounds for the conclusion that the nature of SCC of AISI 4340 steel in water vapour at room temperatures is hydrogen embrittlement via a hydrogen enhanced local plasticity mechanism.

5. Conclusions

- Hydrogen changed the nature of the strain distribution at the crack tip. The effects of hydrogen on the CTOD were small at 5 Torr hydrogen and were significant at a hydrogen pressure of 15 Torr.
- A pressure of 15 Torr of hydrogen at the stress intensity factor of 25 $MPa\sqrt{m}$ resulted in hydrogen enchanced localised plasticity at the crack tip.
- Water vapour produced changes in the plastic behaviour at the crack tip similar to those in a hydrogen atmosphere.

Acknowledgement

This work was supported by the Australian Research Council.

References

1. N. N. KINAEV, D. R. COUSENS and A. ATRENS, The Crack Tip Strain Field for AISI 4340, Part I, Measurement Techniques, *J. Mater. Sci*. **34** (1999) 4909.
2. N. N. KINAEV, D. R. COUSENS and A. ATRENS, The Crack Tip Strain Field for AISI 4340, Part II, Experimental Results, *J. Mater. Sci*. **34** (1999) 4921.
3. J. W. HUTCHINSON, *J. Mech. Phys. Solids* **16** (1968) 337–347.
4. *Idem., ibid*. **16** (1968) 13–31.
5. J. R. RICE and G. F. ROSENGREN, *ibid*. **16** (1968) 1–12.
6. D. L. DAVIDSON, in Proceedings of New Techniques for Characterizing Corrosion and Stress Corrosion (TMS Miner. Metals & Mater. Soc, Warrendale, PA, USA, 1996) pp. 163–174.
7. S. SUN, K. SHIOZAWA, J. GU and N. CHEN, *Metall and Mater. Trans. A* **26A** (1995) 731–739.

Received 25 November 1998
and accepted 15 March 1999